




Open Archive Toulouse Archive Ouverte (OATAO)

OATAO is an open access repository that collects the work of Toulouse researchers and makes it freely available over the web where possible

This is an author's version published in: <http://oatao.univ-toulouse.fr/27436>

Official URL: <https://doi.org/10.1002/ente.201901304>

To cite this version:

Nadeina, Arina and Rozier, Patrick  and Sez nec, Vincent *Facile Synthesis of a Common Na-Ion Battery Cathode Material Na₃V₂(PO₄)₂F₃ by Spark Plasma Sintering.* (2020) *Energy Technology*, 8 (5). 1901304. ISSN 2194-4288

Any correspondence concerning this service should be sent to the repository administrator: tech-oatao@listes-diff.inp-toulouse.fr

Facile Synthesis of a Common Na-Ion Battery Cathode Material $\text{Na}_3\text{V}_2(\text{PO}_4)_2\text{F}_3$ by Spark Plasma Sintering

Arina Nadeina, Patrick Rozier, and Vincent Seznec*

In the pursuit of facile, fast, and efficient methods for the synthesis of various compounds for a variety of applications, spark plasma sintering (SPS) technique is considered to be a powerful and simple tool. Using this technique, a popular cathode material for Na-ion batteries $\text{Na}_3\text{V}_2(\text{PO}_4)_2\text{F}_3$ is synthesized and characterized with X-ray diffraction and scanning electron microscopy (SEM), and is electrochemically tested in Swagelok-type cells in a galvanostatic mode. The obtained material is compared with the conventionally synthesized (via a solid-state route) sample. SEM analysis shows 2 times smaller particles in the case of SPS-synthesized material compared with the solid-state-synthesized material which is to be expected from the fast (40 min in total) SPS synthesis that practically excludes grain/particle growth and promotes much faster diffusion, thereby drastically enhancing the reaction kinetics. Electrochemical performance of the SPS-obtained material shows an improvement in decreasing the overpotential and reducing the capacity loss at high C-rates (8C).

1. Introduction

Increasing demand for renewable energy sources linked to the climate change, global warming, and depletion of natural sources of oil and gas dictates the urge of developing new materials as well as improving the technology and manufacturing process of the already present ones. Na ion batteries (SIBs) have drawn the attention of scientists in the past couple of decades as an alternative to Li ion batteries (LIBs). SIBs have several advantages over LIBs, such as higher safety (could be stored and transported under 0 V), vast abundance, and lower cost of Na and its salts. For that

matter, a lot of research effort has already been put into developing new, safe, high performance electrode materials for SIBs.

$\text{Na}_3\text{V}_2(\text{PO}_4)_2\text{F}_3$ (NVPF) has been considered as one of the very promising cathode materials for SIB due to its high electrochemical stability, good electrochemical performance (theoretical capacity: 128 mAh g^{-1} for 2Na^+ intercalation), and fast ion transport properties.^[1] Since the discovery of its crystal structure in 1999 by Le Meins et al.,^[2] many synthetic routes of pure NVPF and its composites have been proposed and realized,^[3–8] including carbothermal reduction, solid state, hydrothermal, and sol gel (followed by heat treatment) syntheses. Although these methods seem to be rather facile, their duration varies from 8 to 65 h and involves intermediate grindings and a perfectly controlled atmosphere for all

annealing steps. A spray drying method is also reported in the literature,^[9] which is quite fast (takes approximately 4 h, including the heat treatment), but involves a multistep procedure.

Recently, some electrode materials and potential ceramic solid electrolytes for LIBs have been synthesized by means of spark plasma sintering (SPS).^[10–13] SPS utilizes a pulsed direct current along with a uniaxial pressure to create very compact materials in a short time while maintaining an excellent grain to grain bonding and retention of initial particle/grain size.^[14,15] Apart from the obvious simplification of the synthesis route as well as synthesis time reduction, SPS also prevents the possible oxidation of the precursors/final compounds due to the inert (Ar) atmosphere of the sintering chamber, making this method very attractive for a variety of applications.^[10–13,16–18]

In the current work, phase pure bare and carbon coated NVPF (here NVPF_{SPS} and $\text{c NVPF}_{\text{SPS}}$ for bare and carbon coated samples, respectively) have been synthesized in a one step procedure by SPS in only 40 min. The rapidity of the process allows, in addition, to maintain small particle size which promotes better Na ions diffusion, thereby enhancing the electrochemical performances of these samples by showing better capacity and C rate behavior when compared with the conventionally synthesized NVPF (here NVPF_{SS} and $\text{c NVPF}_{\text{SS}}$ for bare and carbon coated samples, respectively).

2. Results and Discussion

2.1. X-Ray Diffraction Analysis and Profile Matching

The comparison of the X ray diffraction (XRD) patterns of the different samples (Figure 1) shows that in all cases the main

A. Nadeina, Dr. V. Seznec
Laboratoire de Réactivité et Chimie des Solides (LRCS)
CNRS UMR 7314
Université de Picardie Jules Verne
33 Rue Saint Leu, Amiens Cedex 80039, France
E mail: vincent.seznec@u-picardie.fr

A. Nadeina, Dr. P. Rozier, Dr. V. Seznec
Réseau sur le Stockage Electrochimique de l'Energie (RS2E)
CNRS FR3459
33 Rue Saint Leu, Amiens Cedex 80039, France

Dr. P. Rozier
CRIMAT
Université de Toulouse
CNRS
Université Toulouse 3 – Paul Sabatier, 118 Route de Narbonne, Toulouse
Cedex 9 31062, France

 The ORCID identification number(s) for the author(s) of this article can be found under <https://doi.org/10.1002/ente.201901304>.

DOI: 10.1002/ente.201901304

compound corresponds to typical NVPF as reported by Bianchini et al.^[19] However, at least one side product, identified as NaVP_2O_7 ^[20] in c-NVPF_{SS} or remaining (c)VPO₄^[21] in NVPF_{SS} and c-NVPF_{SS}, is observed in samples obtained by the typical solid state reaction (Figure 1b), red and black arrows, respectively, while no side products are observed in the samples synthesized by SPS. This clearly shows the specificity of SPS process in enhancing the completeness rate of reactions despite shorter synthesis time (15 vs 120 min in this case).

Profile matching of both bare and carbon coated NVPF samples has been performed. Apart from specific background due to the sample holder, it confirms the successful synthesis of NVPF (Space Group: Amam) with refined lattice parameters (Table 1) close to reported values.^[19]

Rietveld refinement of SPS synthesized samples could be found under the SI 2 in Supporting Information. Rietveld analysis of the XRD patterns does not allow to evidence the decrease in the orthorhombic distortion (b/a ratio is ≈ 1.002 , correlates well with reported in the literature^[22] for $\text{Na}_3\text{V}_2(\text{PO}_4)\text{F}_{3-\gamma}\text{O}_\gamma$ with $\gamma=0$ (no oxygen substitution onto the fluorine sites)) of the obtained NVPF samples suggesting the absence of O/F mixing.

2.2. Scanning Electron Microscopy

The analysis of particle size and shape was performed by means of scanning electron microscopy (SEM) and compared with the initial particle size of (c)VPO₄ (Figure 2). All samples

Table 1. Lattice parameters of obtained samples refined using *profile matching* and reported values for NVPF.

Sample	Lattice parameters [Å]		
	<i>a</i>	<i>b</i>	<i>c</i>
NVPF _{SS}	9.0300(5)	9.0441(1)	10.7521(1)
c-NVPF _{SS}	9.0299(4)	9.0462(4)	10.7596(3)
NVPF _{SPS}	9.0277(3)	9.0406(3)	10.7475(2)
c-NVPF _{SPS}	9.0273(3)	9.0413(3)	10.7486(2)
NVPF ^[19]	9.02847(3)	9.04444(3)	10.74666(6)

were analyzed in a high vacuum mode, with 20 kV accelerating voltage, and secondary electrons detection mode. Particle size distribution analysis was performed by means of *ImageJ2* software.^[23]

The mean particle size of bare NVPF obtained by the solid state synthesis is around 240 nm, while SPS synthesized sample has the mean value of 150 nm. A difference in particle size of c-NVPF_{SS} and c-NVPF_{SPS} is also observed resulting in 2 times smaller particles for the latest (450 vs 230 nm, respectively). The obvious difference of the particle size between the bare and carbon coated NVPF samples (both solid state synthesized and SPS synthesized) results from the initial size of (c)VPO₄ precursors, as shown in Figure 2e-f. Smaller particle size in case of SPS synthesized samples results from the rapidity of the SPS

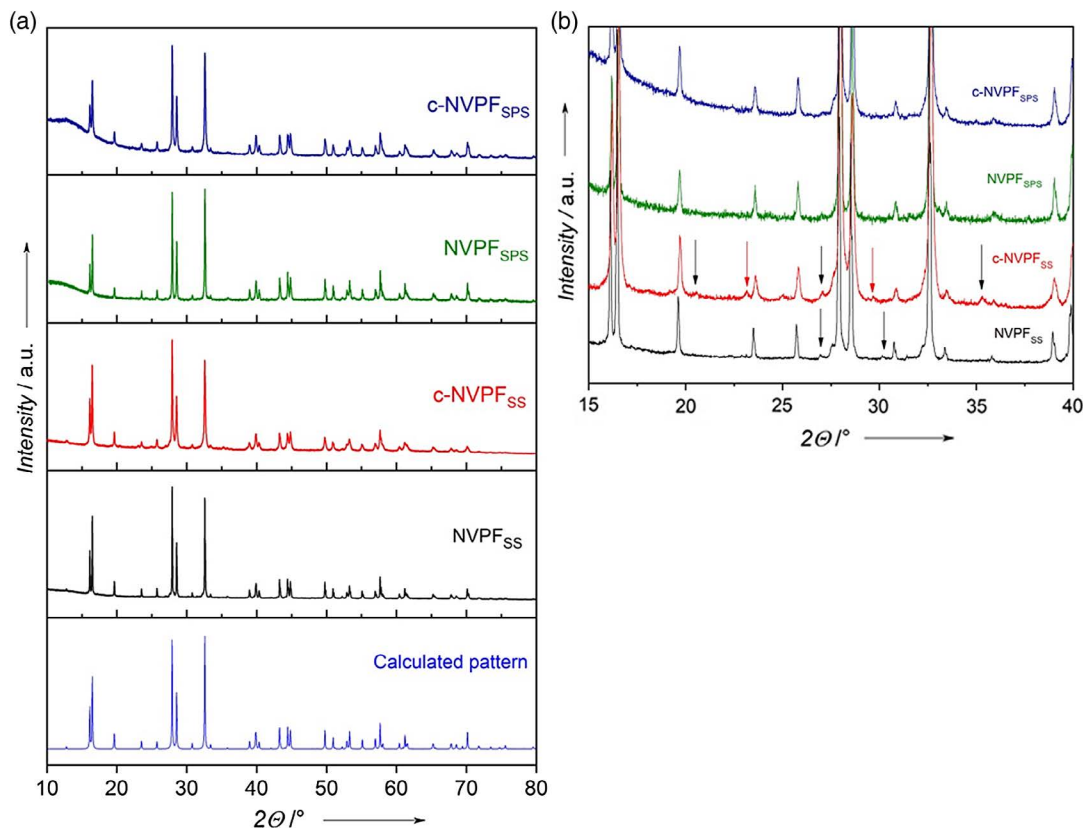


Figure 1. a) XRD patterns of NVPF_{SS}, c-NVPF_{SS}, NVPF_{SPS}, and c-NVPF_{SPS}. b) Selected area for NVPF_{SS}, c-NVPF_{SS}, NVPF_{SPS}, and c-NVPF_{SPS}.

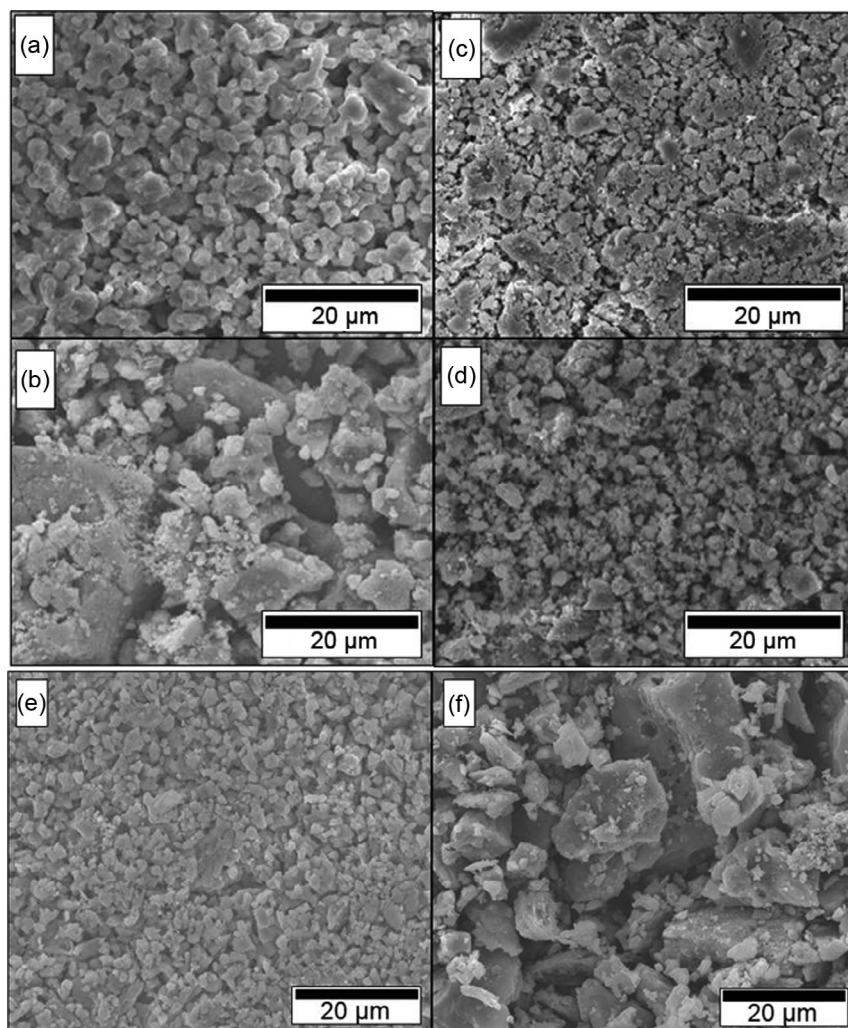


Figure 2. SEM images of NVPF: a) NVPF_{SS}, b) c NVPF_{SS}, c) NVPF_{SPS}, d) c NVPF_{SPS}, e) bare VPO₄, and f) c VPO₄.

procedure yielding little to no particle growth proving a high efficiency of such synthesis technique, especially when maintaining the small particle size is crucial or beneficial for the future applications.

2.3. Electrochemical Performance

SPS synthesized samples of bare and carbon coated NVPF were compared in terms of electrochemical performance with solid state synthesized carbon coated NVPF (**Figure 3**) at different C rates (here 1C rate is determined as the exchange of 1 sodium ion/1 h).

Bare NVPF synthesized by SPS (Figure 3a) shows the typical electrochemical signature with two plateaus at 3.5 and 4.2 V.^[19,24] The first charge capacity at C/10 is close to 80 mAh g⁻¹ (compared with 130 mAh g⁻¹ as reported in ref. [24]). Upon increasing the charge/discharge rate up to 8C, the reversible charge/discharge capacities fade drastically which is to be expected from the cell setup (cycling of powder) as well as from the absence of carbon coating.^[25,26] Nonetheless, after

40 cycles, the capacity retention at C/10 is 92.8%, indicating good reaction reversibility.

Contrary to bare NVPF_{SPS}, both c NVPF_{SPS} and c NVPF_{SS} deliver 121 and 126 mAh g⁻¹ on the first charge, respectively (Figure 3b,c), which correlates very well with the theoretical capacity of 128 mAh g⁻¹ (for intercalation of two sodium ions per formula unit). With an increase of cycling rates (up to 8C), the reduction of the capacity loss, as well as the decrease in overpotential, is observed for carbon coated NVPF, both solid state synthesized and SPS synthesized, as compared with the bare NVPF. In the case of c NVPF_{SS}, the delivered discharge capacity at the end of 8C cycles results in ≈40 mAh g⁻¹, while in the case of c NVPF_{SPS} it yields ≈71 mAh g⁻¹. This type of behavior of carbon coated NVPF samples is anticipated as carbon coating improves the intrinsically poor electronic properties of NVPF resulting in decreased overpotential and better overall performance at higher C rates.^[25,26] Lower overpotential and reduced capacity loss of c NVPF_{SPS} compared with solid state synthesized c NVPF could be explained by smaller particle sizes in case of c NVPF_{SPS} and more homogeneous carbon coating. Both

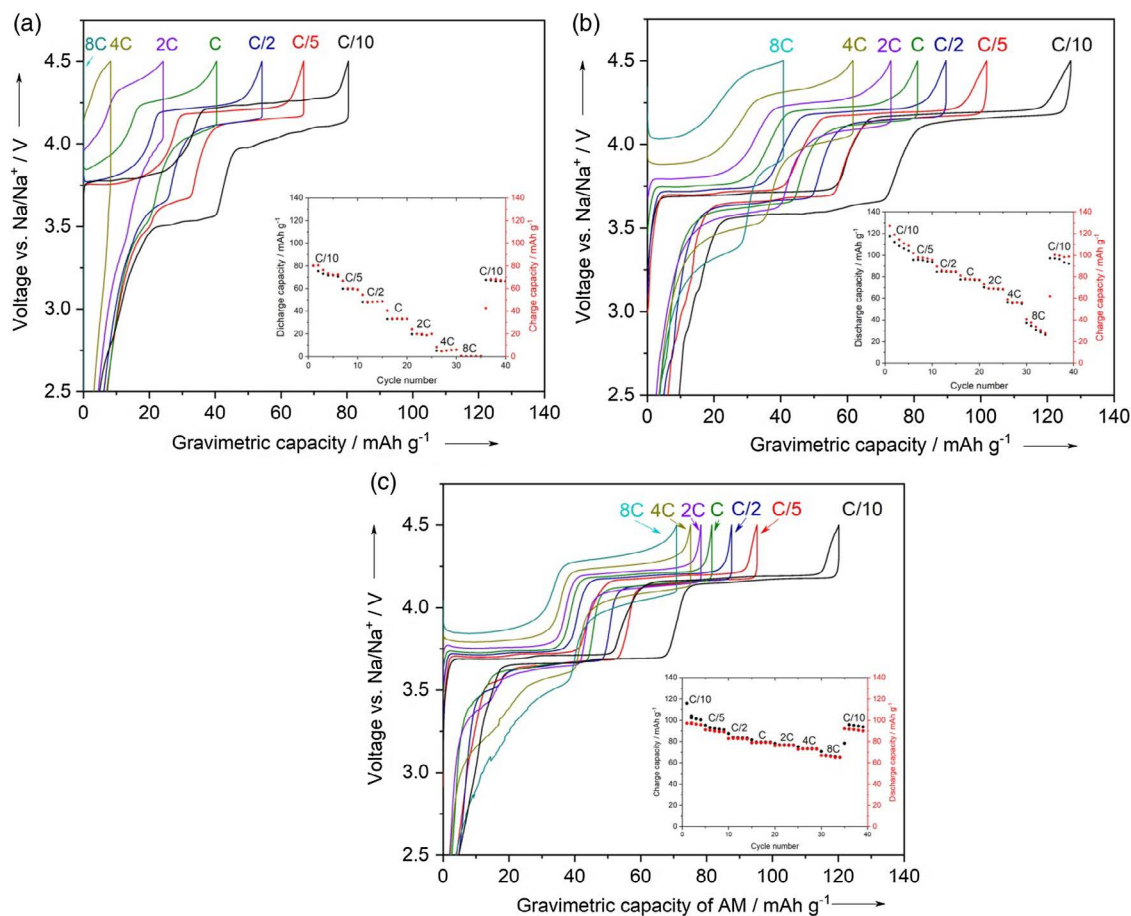


Figure 3. Galvanostatic charge discharge profiles of NVPF samples versus sodium metal under different C rates with rate capability graphs shown in insets for a) bare NVPF_{SPS}, b) NVPF_{SS}, and c) c NVPF_{SPS}.

compounds show good capacity retention after 40 cycles, yielding 90% and 91% for c NVPF_{SS} and c NVPF_{SPS}, respectively, which indicates good electrochemical stability of the cycled compounds even after cycling at high C rates. In addition, one cannot note any changes in the shape of the cycling profiles (such as smoothing) which, along with XRD and Rietveld refinement data, confirms the absence of the partial substitution of fluorine by oxygen.^[22]

3. Conclusions

SPS has once again proven itself to be a very efficient tool toward not only sintering but also synthesis of different families of materials, including phase pure electrode materials for LIBs and SIBs. By its means, phase pure NVPF has been synthesized in a remarkably short time (40 min vs 10 h of solid state reaction). Obtained material shows good electrochemical performance when compared with the conventionally synthesized sample.

Moreover, SPS could be adopted for the synthesis of air sensitive materials, materials with high reaction temperatures as well as for materials when maintaining the small particle size is crucial. Fine tuning of SPS parameters could allow the “scale up” one step synthesis of various compounds making it attractive for the future commercial application.

4. Experimental Section

Synthesis: NVPF has been synthesized using commercial NaF (Sigma Aldrich, $\geq 99\%$) and homemade VPO₄ or carbon coated VPO₄ (c VPO₄). VPO₄ and c VPO₄ were synthesized by the same sol gel method.^[27] H₃PO₄ (Sigma Aldrich, $\geq 99.0\%$) was dissolved in deionized water under stirring for 20 min. Stoichiometric amount of V₂O₅ (Alfa Aesar, 99.6%) only or together with agar agar (Fisher BioReagents) as carbon source (22 wt% of the mixture H₃PO₄ + V₂O₅) were added for the synthesis of VPO₄ or c VPO₄, respectively. The mixture was heated up to 85 °C under ambient conditions, stirred to ensure compounds dissolution, and then heated up to 250 °C for 2 h until complete solvent evaporation. The obtained powder was ground in a mortar and heated under Ar atmosphere with 5 °C min⁻¹ rate up to 890 °C (dwell time: 2 h).

Stoichiometric mixture of NaF and as prepared VPO₄ or c VPO₄ was ball milled for 30 min using a SPEX Mixer Mill 8000M, and two different processes, namely, solid state route and reactive sintering by SPS, were used to synthesize NVPF. The typical solid state synthesis route consisted of heat treatment of the mixture in an alumina crucible under Ar atmosphere at 750 °C for 2 h (heating/cooling rate: 3 °C min⁻¹)^[24] with a subsequent grinding of the obtained powder in a mortar for 30 min.

For the SPS synthesis, the mixture was packed into a graphite die (10 mm inner diameter) preliminary lined with graphite paper, placed in the chamber of FCT GmbH HPD10 which was evacuated down to 10⁻³ Pa. Then the sample was heated from 25 to 750 °C within 10 min (corresponding heating rate: 75 °C min⁻¹) with direct current pulses of

1 ms followed by 1 ms rest time (delivering power restricted to 80% of the maximal value of 37 kW) while simultaneously increasing the force to 10 kN. In line, a dwell step at 750 °C for 15 min while increasing the force to 11 kN was realized, followed by a controlled cooling within 10 min down to the room temperature (total synthesis/sintering time: 40 min). The obtained pellets were polished to remove the graphite paper and then ground in a mortar for 30 min to get a fine powder.

Characterization: The phase composition was investigated by XRD diffraction on a D4 Endeavor Bruker diffractometer (Cu K α radiation, $\lambda = 1.5418 \text{ \AA}$), the XRD patterns were recorded in the $10^\circ - 80^\circ 2\theta$ range with 0.02° angular step and 5 s counting time, and profile matching using the FullProf Suite was performed. Particle shape/size was analyzed by SEM on a FEI Quanta 200F field emission scanning electron microscope. For the SEM analysis, to avoid overcharging, all samples were covered by a thin film of gold sputtered using Sputter Coater Bal Tec SCD 050. Electrochemical performances of the obtained materials were tested in a galvanostatic mode using a Biologic VMP 3 (Biologic SAS, France) instrument with a voltage window 2.5–4.5 V. Swagelok cells were assembled with mortar ground (c) NVPF + 15 wt% carbon C 45 as a cathode, NaPF₆ in 1:1 wt% EC:DMC with 3% fluoroethylene carbonate (FEC) as an electrolyte.

Supporting Information

Supporting Information is available from the Wiley Online Library or from the author.

Acknowledgements

The authors acknowledge Carlos Alarson and Francois Rabuel for their contribution to the article by synthesizing (c) VPO₄ and (c) NVPF_{ss} samples. This work was funded by LABEX STOREX and is made within the French Research Network on Electrochemical Energy Storage (RS2E), National Center for Scientific Research (CNRS).

Conflict of Interest

The authors declare no conflict of interest.

Keywords

cathode materials, sodium ion batteries, solid state synthesis, spark plasma sintering

- [1] W. Song, X. Cao, Z. Wu, J. Chen, Y. Zhu, H. Hou, Q. Lan, X. Ji, *Langmuir* **2014**, *30*, 12438.
- [2] J. M. Le Meins, M. P. Crosnier Lopez, A. Hemon Ribaud, G. Courbion, *J. Solid State Chem.* **1999**, *148*, 260.
- [3] R. K. B. Gover, A. Bryan, P. Burns, J. Barker, *Solid State Ionics* **2006**, *177*, 1495.
- [4] Z. Liu, Y. Y. Hu, M. T. Dunstan, H. Huo, X. Hao, H. Zou, G. Zhong, Y. Yang, C. P. Grey, *Chem. Mater.* **2014**, *26*, 2513.
- [5] W. Song, S. Liu, *Solid State Sci.* **2013**, *15*, 1.
- [6] R. A. Shakoor, D. H. Seo, H. Kim, Y. U. Park, J. Kim, S. W. Kim, H. Gwon, S. Lee, K. Kang, *J. Mater. Chem.* **2012**, *22*, 20535.
- [7] T. Jiang, G. Chen, A. Li, C. Wang, Y. Wei, *J. Alloys Compd.* **2009**, *478*, 604.
- [8] J. Barker, R. K. B. Gover, P. Burns, A. J. Bryan, *Electrochem. Solid State Lett.* **2006**, *9*, A190.
- [9] N. Eshraghi, S. Caes, A. Mahmoud, R. Cloots, B. Vertruyen, F. Boschini, *Electrochim. Acta* **2017**, *228*, 319.
- [10] E. Dumont Botto, C. Bourbon, S. Patoux, P. Rozier, M. Dolle, *J. Power Sources* **2011**, *196*, 2274.
- [11] Y. Arachi, Y. Higuchi, R. Nakamura, Y. Takagi, M. Tabuchi, *J. Power Sources* **2013**, *244*, 631.
- [12] M. Kotobuki, M. Koishi, *Int. J. Electroact. Mater.* **2014**, *2*, 17.
- [13] Y. X. Gao, X. P. Wang, Q. X. Sun, Z. Zhuang, Q. F. Fang, *Front. Mater. Sci.* **2012**, *6*, 216.
- [14] R. Kali, A. Mukhopadhyay, *J. Power Sources* **2014**, *247*, 920.
- [15] M. Suarez, A. Fernandez, J. L. Menendez, R. Torrecillas, H. U. Kessel, J. Hennicke, R. Kirchner, T. Kessel, *Sintering Appl.* **2013**, <https://doi.org/10.5772/53706>.
- [16] F. Chen, *Mater. Chem. Phys.* **2008**, *86*, 1962.
- [17] S. Choudhary, S. Singhal, M. Srivastava, P. Jain, V. Yadav, *Int. J. Sci. Eng. Res.* **2012**, *3*, 1.
- [18] C. Yu, T. J. Zhu, R. Z. Shi, Y. Zhang, X. B. Zhao, J. He, *Acta Mater.* **2009**, *57*, 2757.
- [19] M. Bianchini, F. Fauth, N. Brisset, F. Weill, E. Suard, C. Masquelier, L. Croguennec, *Chem. Mater.* **2015**, *27*, 3009.
- [20] Y. P. Wang, K. H. Lii, S. L. Wang, *Acta Crystallogr. C Cryst. Struct. Commun.* **1989**, *45*, 1417.
- [21] R. Glaum, R. Gruehn, *Zeitschrift fuer Kristallographie* **1992**, *198*, 41–47.
- [22] T. Broux, T. Bamine, F. Fauth, L. Simonelli, W. Olszewski, C. Marini, M. Ménétrier, D. Carlier, C. Masquelier, L. Croguennec, *Chem. Mater.* **2016**, *28*, 7683.
- [23] C. T. Rueden, J. Schindelin, M. C. Hiner, B. E. Dezonio, A. E. Walter, E. T. Arena, K. W. Eliceiri, *BMC Bioinf.* **2017**, *18*, 529.
- [24] T. Broux, F. Fauth, N. Hall, Y. Chatillon, M. Bianchini, T. Bamine, J. Leriche, E. Suard, D. Carlier, Y. Reynier, L. Simonin, *Small Methods* **2019**, *3*, 1800215.
- [25] C. Zhu, C. Wu, C. C. Chen, P. Kopold, P. A. Van Aken, J. Maier, Y. Yu, *Chem. Mater.* **2017**, *29*, 5207.
- [26] Q. Liu, D. Wang, X. Yang, N. Chen, C. Wang, X. Bie, Y. Wei, G. Chen, F. Du, *J. Mater. Chem. A* **2015**, *3*, 21478.
- [27] R. David, C. Surcin, M. Morcrette, *France Patent WO2018/142082A1*, **2018**.